

---

## 2-3 Research on Superconductive Oscillators and Detectors at Terahertz Frequency Regions

WANG Zhen, KAWAKAMI Akira, and UZAWA Yoshinori

Development of generating and detecting technology in the THz frequency region is an important subject for high-speed telecommunication technology in the future. Recently, it is necessary to develop THz-band oscillators and detectors in the field of globe environment measurements and radio physics. We have developed superconducting Josephson array oscillators and low-noise SIS mixers for THz-band solid oscillator and highly sensitive detector. In this paper, we show oscillating properties and frequency dependence of output for 650 GHz and 1 THz Josephson array oscillator, and discuss low-noise properties of 800 GHz-band SIS mixers.

### *Keywords*

Terahertz frequency, Superconductivity, Josephson junction, Array oscillator, SIS mixer

### 1 Introduction

The terahertz band, located between the electromagnetic and lightwave bands, remains relatively unexplored in terms of wave-generation and detection applications. For example, the only oscillators currently operable in frequency ranges over 1 THz are submillimeter wave lasers and BWOs (backward wave oscillators). There are no highly stable, solid-state oscillators with long lifetimes (such as semiconductor frequency multipliers, for example). Moreover, in terms of detectors, the semiconductor bolometers developed to date offer only slow response. In a number of fields, from global environmental measurement to radio astronomy, a growing need is seen for a highly sensitive, rapid heterodyne detector device.

The Josephson junction—in which two superconductive materials are weakly coupled through an insulator, an electrical conductor, or a superconductive material—produces very

strong non-linearity due to its coherent operation (coherence of wave-function phases), and is expected to serve as an electronic device featuring extremely high frequency and rapid operation. However, because superconductive materials used are made of multiple elements and the superconducting coherence length is short, deposition of thin films and fabrication of Josephson junctions become quite difficult. For example, in producing a Josephson junction with a single-value current-phase relationship, the junction component must be of a size on the order of the superconducting coherence length (a few nanometers), which requires growth of atomic-level layered thin films, nanometer-scale interface control technology, and sub-micron micromachining technology. Further, as the superconductivity transition temperature ( $T_c$ ) increases, the coherence length becomes extremely short, and device construction is rendered even more difficult. As a result, for the 30 years since the discovery of the Josephson effect, the only supercon-

ducting technology put into practice consists of the tunnel junction using superconductive materials of lead alloys, metal niobium (Nb), and the like, with application only to limited fields.

The current study is aimed at the practical development of a superconducting device operating in the terahertz frequency, through research into a superconducting Josephson array oscillator and a low-noise SIS mixer that takes advantage of the excellent electromagnetic properties of the superconducting device. This paper describes the production of a terahertz-band superconducting oscillator and a detector, discusses the operating properties of 650-GHz and 1-THz Josephson array oscillators, and evaluates the performance of an 800-GHz SIS mixer, among others.

## 2 Josephson array oscillator

The Josephson array oscillator makes use of the alternating-current Josephson effect of a superconducting Josephson junction, and is capable of generating a high-frequency oscillating current whose frequency (approximately 484 GHz/mV) is in proportion to an applied direct current voltage. It is known, however, that the oscillation output of a Josephson junction is only a few nanowatts and that the oscillation line width is wide (a few hundreds of MHz)[1]. To obtain a practical oscillation output (i.e., greater than several microwatts) and useful oscillation line width, in this study we designed a Josephson array oscillator composed of multiple Josephson junctions with synchronized phases. We then produced an experimental model and evaluated its performance[2][3].

### 2.1 Thin-film-resistance-shunted Nb/AlOx/Nb tunneling Josephson junction

Generally, the tunneling Josephson junctions used in Josephson array oscillators excel in uniformity, reproducibility, and other properties. However, when a LCR resonant circuit formed of a thin-film resistance is added to the

structure of such a junction, the output impedance of the junction exhibits clear frequency dependence, and the real part of the impedance (complex number) drops rapidly at frequencies equal to or higher than the resonance frequency[5]. In the case of the general thin-film-resistance-shunted Josephson junction, the resonance frequency lies in the vicinity of several hundred GHz, which does not present a problem in applications at frequencies less than this, as is the case with a SQUID fluxmeter. However, in high-frequency applications such as those associated with the Josephson oscillator, this resonance property affects the upper limit oscillation frequency and output impedance; therefore, it is extremely important to assess these properties precisely. In particular, for the Josephson oscillator oscillating and operating in the submillimeter frequency range, it is necessary to develop a thin-film-resistance-shunted tunneling Josephson junction having excellent high-frequency properties. In this study, we proposed a structure for a thin-film-resistance-shunted tunneling Josephson junction capable of operating in the THz band, and applied computer simulation to evaluate the high-frequency properties of an actual such Josephson junction.

Figure 1(a) shows a microphotograph of the thin-film-resistance-shunted Josephson junction produced using the conventional manufacturing process. Although this type of junction excels in homogeneity and reproducibility and offers improved high-frequency characteristics relative to only a single tunnel junction, parasitic inductance ( $L_s$ ) is formed by the added thin-film resistance. Accordingly, this parasitic inductance constitutes a resonant structure, and the high-frequency response of the Josephson junction is limited by this resonance.

In order to improve the high-frequency properties of the thin-film-resistance-shunted Josephson junction, the product of  $L_s$  and  $C_j$  must be smaller. However, because the oscillation output in the Josephson oscillator depends on the junction critical current, there is a limit to the reduction in junction capaci-

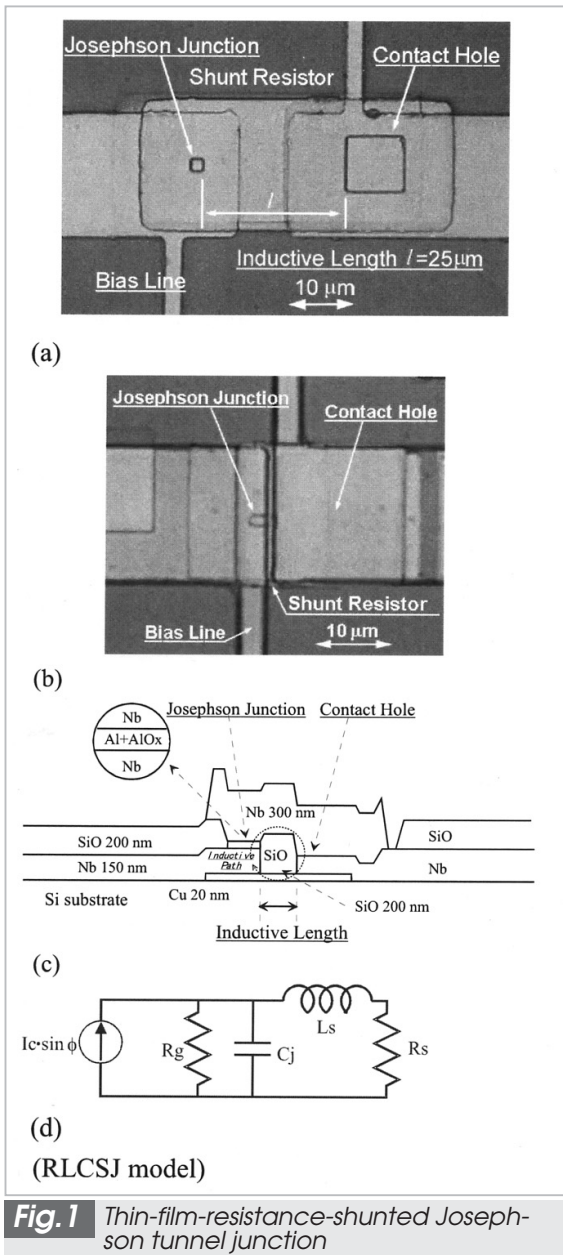


**Fig. 1** Thin-film-resistance-shunted Josephson tunnel junction

tance  $C_j$  (this capacitance is in proportion to the junction critical current) while maintaining oscillation output; minimization of parasitic inductance  $L_s$  is thus critical. Because parasitic inductance  $L_s$  depends on the distance between the junction and contact hole, we tried to minimize parasitic inductance by reducing this distance (i.e., the inductive length) from approximately  $25 \mu\text{m}$ , the conventional value, to  $1 \mu\text{m}$ , nearly the limit value in the present process. Figure 1(b) shows a microphotograph of a device subject to such minimization of parasitic inductance, while (c)

shows a cross-sectional view of this device. Figure 1(d) shows an equivalent circuit of the thin-film-resistance-shunted Josephson junction which has a resonance-generating structure (RLCSJ model). Here,  $I_c$ ,  $R_s$ , and  $R_g$  denote the critical current, the thin film resistance, and resistance in gap voltage in the tunnel junction, respectively. This junction achieved a distance between the junction and contact hole of approximately  $1 \mu\text{m}$  thanks to the formation of a part of the tunnel junction at the time of lithography when the junction determines the thin-film resistance length.

Figure 2 shows the current-voltage characteristics and the  $(I - I_{RSJ}) - V$  characteristics of the thin-film-resistance-shunted Josephson junction shown in Fig.1(b). The difference between measured values and simulation results using the RLCSJ model is not shown in these current-voltage characteristics. Therefore, a case without a resonant structure (RSJ model) was calculated based on the measured junction parameters, the only observed  $(I - I_{RSJ}) - V$  characteristic seen is the resonance-induced increase in direct current. Based on this characteristic, an increase in the direct current centering near  $1.3 \text{ mV}$  was recognized, indicating that the resonance occurred at approximately  $630 \text{ GHz}$ . Comparing the results of actual measurement with those of simulation using the RLCSJ model, parasitic inductance was estimated at approximately  $100 \text{ fH}$ . The parasitic inductance  $L_s$  of the thin-film-resistance-shunted Josephson junction in Fig.1(a) was already estimated at approximately  $1 \text{ pH}$ [2], indicating that parasitic inductance was reduced to one-tenth of the conventional value.

## 2.2 Design and production of array oscillator

The developed Josephson array oscillator consists of an oscillator, composed of a microstrip resonator and a Josephson junction, and a detector, composed of a matching load and a Josephson junction to detect current. Figure 3 shows a microphotograph of the experimental  $650\text{-GHz}$  band Josephson array

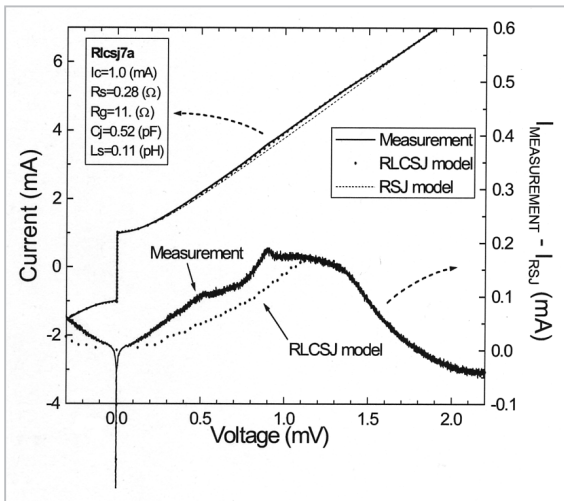


**Fig.2** Current-voltage characteristics and  $(I - I_{RSJ}) - V$  characteristics of the thin-film-resistance-shunted Josephson junction

oscillator. A Nb microstrip line  $20 \mu\text{m}$  wide constituting the resonator is formed under the SiO dielectric thin film (thickness of  $1 \mu\text{m}$ ) below the Nb ground plane. Here, the film thicknesses of the microstrip line and of the ground plane were each set to  $150 \text{ nm}$ ; significantly thicker than the magnetic penetration depth. The Josephson junctions were arranged in an array along the microstrip line at every half-wavelength, with a total of 11 junctions. In this study, two kinds of predetermined oscillator frequencies,  $650 \text{ GHz}$  and  $1 \text{ THz}$ , were established, and line wavelengths were approximately  $180 \mu\text{m}$  and  $12 \mu\text{m}$ , respectively. The characteristic impedance of the microstrip line was approximately  $8 \Omega$ .

The right end of the oscillator has a quarter-wave stub through which the Josephson array makes a short circuit to the ground at a designated high frequency. The other end of the oscillator is connected to a detector through

a Nb microstrip line  $5\text{-}\mu\text{m}$  wide featuring characteristic impedance of  $32 \Omega$ . Impedance mismatching of the line connecting the oscillator to the detecting component reduces the effect on the oscillator of variation in load-side impedance. The detector is composed of a matching load made of a Cu microstrip line (featuring the same characteristic impedance as that of  $5\text{-}\mu\text{m}$ -wide Nb line) and a Josephson junction to detect oscillation output. The oscillation output from the oscillator passes through the coupling element, which applies impedance mismatching, passes through the Josephson junction detector and then propagates to the Cu microstrip line. The Cu surface resistance is set such that the propagating signal is subject to attenuation loss of approximately  $-40 \text{ dB}$  or more over the course of a round trip through the  $400\text{-}\mu\text{m}$  Cu line; consequently the Cu microstrip line can be regarded as a matching load.

The DC bias line constitutes a low-pass filter in which microstrip lines  $4 \mu\text{m}$  and  $20 \mu\text{m}$  wide are positioned at every quarter-wave. Therefore, the DC bias line becomes a high-impedance line and can be ignored at the design frequency. Through this arrangement, each Josephson junction constituting the array operates as if connected serially at high frequencies and operates as if connected in parallel when DC bias is applied.

### 2.3 Oscillator performance evaluation

The current-voltage characteristics of the  $650\text{-GHz}$  band Josephson array oscillator are shown in Fig.4. Since the observed oscillator consists of 11 Josephson junctions connected to each other in parallel, the critical current for one junction  $I_c$  was approximately  $2.1 \text{ mA}$  and

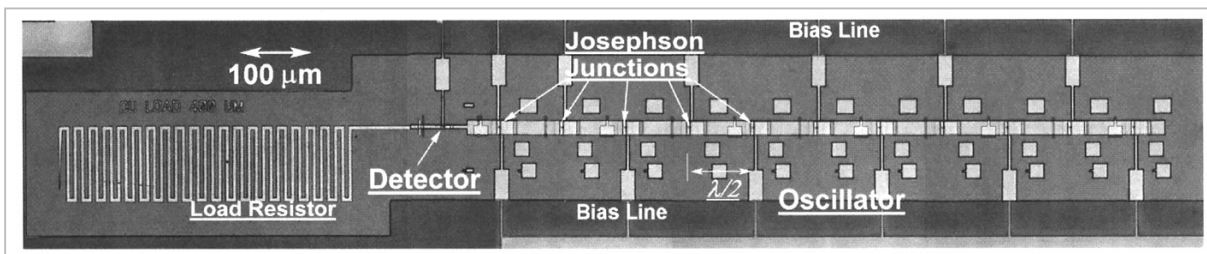


**Fig.3**  $650\text{-GHz}$  band Josephson array oscillator

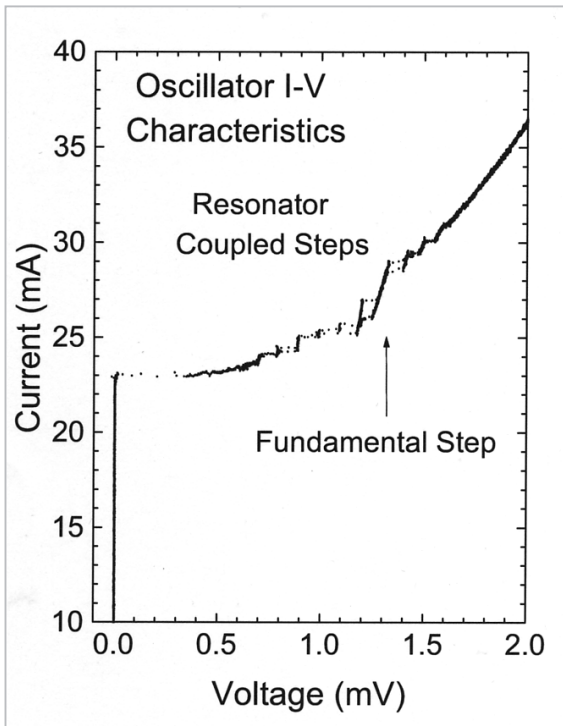


**Fig.4** Current-voltage characteristics of 650-GHz band Josephson array oscillator

the junction capacitance  $C_j$  (estimated from a junction area of approximately  $4 \mu\text{m}^2$ ) was 0.5 pF. Assuming that parasitic inductance  $L_s$  is 100 fH, the resonance frequency of the junction element becomes approximately 700 GHz, and thus the oscillator is considered to work sufficiently well at the oscillator design frequency. In terms of current-voltage characteristics, a current step (i.e., a fundamental step) caused by design resonance of the microstrip resonator can be observed at a voltage of approximately 1.3 mV. Within this current step, 11 Josephson junctions are considered to be in a state of phase synchronization, and it is estimated that the maximum oscillation output is obtained when the current bias is set within this step.

Figure 5 shows the current-voltage characteristics of the Josephson junction detector when a DC bias is applied to the oscillator. With the application of a DC bias to the oscillator inducing oscillation, the critical current of the Josephson junction detector was suppressed, and a microwave-induced step (known as a Shapiro step) was observed. The simulation results in the figure were calculated

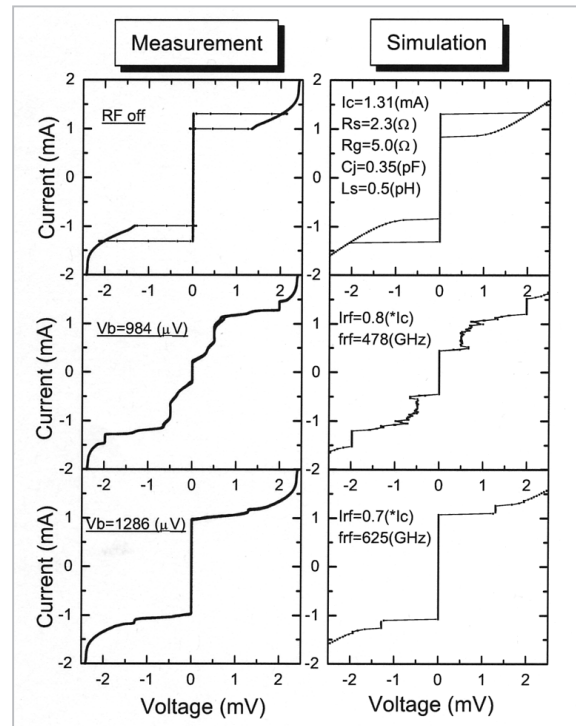


**Fig.5** Current-voltage characteristics of Josephson junction detector

using actually measured parameters of the Josephson junction detector. By comparing actual current-voltage characteristics with the results of simulation, the high-frequency current  $I_{rf}$  flowing in the Josephson junction can be derived. Oscillation frequencies of 478 GHz and 625 GHz yielded values of  $0.8 \times I_c$  and  $0.7 \times I_c$ , where  $I_c$  is the critical current of the Josephson junction detector.

Since the load impedance viewed from the Josephson junction detector exhibits slight frequency dependence everywhere except at the design frequency, it is necessary to take frequency dependence of the load into consideration when evaluating oscillation output. The oscillation output of the Josephson oscillator consumed in the detecting element can be obtained from the estimated high-frequency current  $I_{rf}$  by taking the frequency dependence of the load into consideration. Figure 6 shows the frequency dependence of the oscillation output. This output was observed discretely at voltage intervals corresponding to the current steps in the frequency range from 450 to 900 GHz, and an approximately 10- $\mu\text{W}$  oscillation output was observed at 625 GHz,

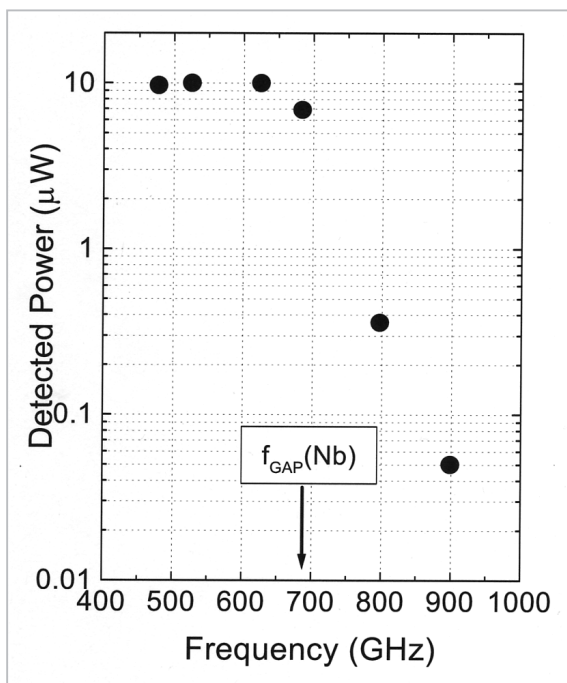


**Fig.6** Frequency dependence of oscillation output

near the designed frequency.

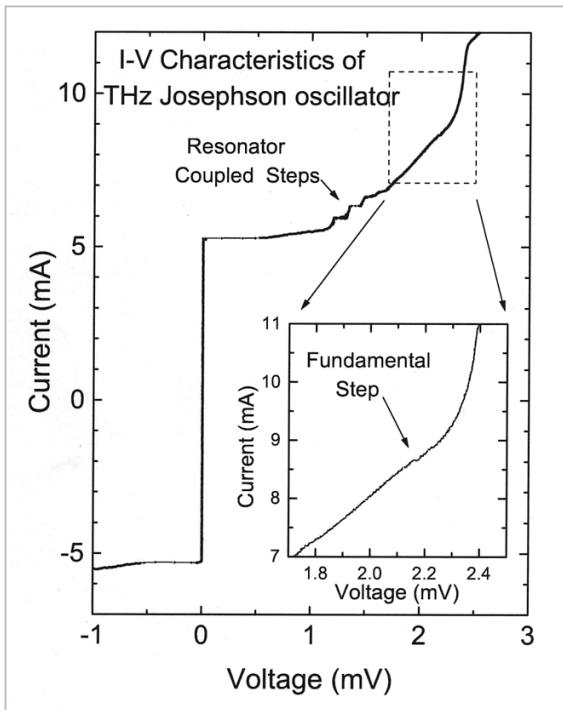
Frequency properties reveal that the obtained oscillation output decreases rapidly from around 700 GHz. Moreover, Fig.4 indicates that for voltages equal to or greater than 1.45 mV corresponding to 700 GHz, the resonator coupled step becomes obscure and tends to attenuate. This frequency corresponds to the energy gap frequency of Nb, a superconductive material; it is therefore expected that at frequencies above 700 GHz, surface resistance loss of the Nb thin film will increase due to the pair-breaking effect in the Nb. We may also conclude that the increase in the resistance loss of the microstrip resonator is one of the main factors leading to the reduction in oscillation output. We believe that it will be possible to construct a THz-band Josephson oscillator delivering practical oscillation output by reducing the surface resistance loss using a thin NbN or Nb<sub>3</sub>Ge film (featuring higher energy gaps than Nb) or using a high-purity metal such as Al or Au for effective use in the THz band.

Figure 7 shows the current-voltage characteristics of the experimental 1-THz Josephson array oscillator. The junction area of the

Josephson junction constituting the oscillator was set to approximately  $1 \mu\text{m}^2$ . The junction capacitance  $C_j$  was estimated at 0.12 pF based on a junction critical current density of approximately  $50 \text{ kA/cm}^2$ [8]. If the parasitic inductance is then assumed to be 100 fH, the junction resonance frequency becomes approximately 1.4 THz; this junction is therefore considered to offer sufficient impedance at the design frequency. Among the current-voltage characteristics, a current step (fundamental step) is observed at approximately 2.1 mV, although the step is only a slight change. Figure 8 shows current-voltage characteristics when the DC bias is set near this step, i.e., to a voltage of 2.06 mV. A clear Shapiro step can be recognized at a voltage of 2.06 mV. This voltage corresponds to 1 THz, and signifies that a 1-THz oscillation output from the oscillator was confirmed by the detector. Comparing the measured Shapiro step with the simulation results, the 1-THz high-frequency current  $I_{rf}$  that flowed in the Josephson junction detector was found to correspond to  $0.1 \times I_c$ ; the oscillation output consumed in the Cu matched resistance of the detection element was estimated as approximately 50 nW. There have been no reports indicating oscillation of the Josephson oscillator beyond 1 THz; the oscillation frequency of the Josephson oscillator described in this paper is thus the highest reported to date.

### 3 Terahertz-band highly sensitive SIS mixer

Since mixers using a superconductor-insulator-superconductor (SIS) tunnel junction offer extremely low noise (close to the quantum noise limit) in the frequency band from millimeter waves to submillimeter waves, these mixers are widely used in fields such as radio astronomy and global environmental measurement[4]. The SIS junction features significant structural electrostatic capacitance, and as such provides a short circuit to high-frequency signals. Therefore, in order to couple an input signal with this junction efficient-



**Fig.7** Current-voltage characteristics of 1-THz Josephson array oscillator

ly, it is necessary to reduce the junction size and also to integrate a tuning circuit to remove junction capacitance. In conventional tuning circuits featuring this structure, the ratio of tunable bandwidth  $\Delta f/f_0$  is limited by  $1/\omega C_J R_N$  of the junction[5]. Here,  $\omega$  denotes angular frequency,  $C_J$  the electrostatic capacitance of

the junction, and  $R_N$  normal resistance. Consequently, in order to secure a bandwidth ratio of 20%, the  $\omega C_J R_N$  product must be approximately 5 at its center frequency. The  $\omega C_J R_N$  product depends strongly on the critical current density  $J_C$  of the junction, and is related to the critical current density  $J_C$  by the following formula[5].

$$J_C = \omega C_J I_C R_N / (\omega C_J R_N) \quad (1)$$

where  $C_S$  is the electrostatic capacitance per unit area of the junction and  $I_C$  is the critical current. For example, assuming that the junction capacitance per unit area is  $100 \text{ f}/\mu\text{m}^2$ , it is necessary to achieve a high critical current density of approximately  $20 \text{ kA}/\text{cm}^2$  in the case of the Nb junction, and of approximately  $40 \text{ kA}/\text{cm}^2$  in the case of NbN junction at a frequency of 1 THz. With the currently available technology, the electrical properties of fabricated junctions tend to deteriorate with increasing critical current density in the junction, which in turn contributes to an increase in noise temperature due to the sub-gap leak current. Furthermore, the tuning circuit becomes short in the super-high frequency range of extremely short wavelengths (such as 1 THz), while reductions in scale are difficult with conventional design techniques; further,

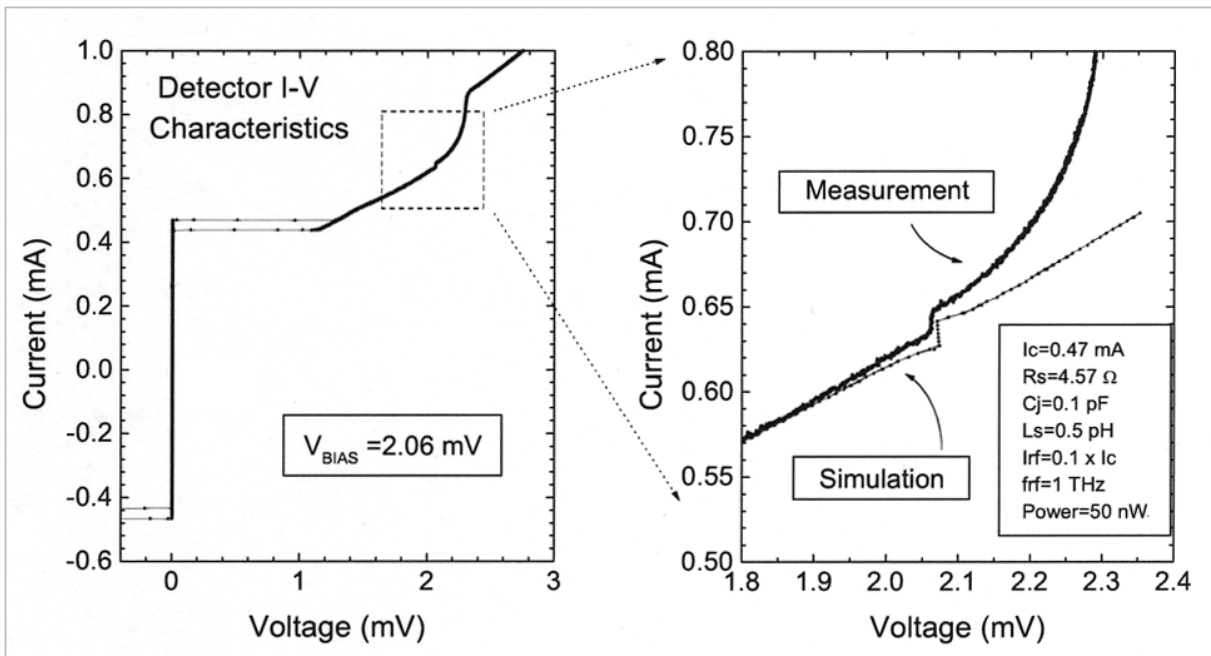


**Fig.8** 1-THz Shapiro step by Josephson oscillation

junction size must be reduced to a size of approximately sub-micrometer. It has therefore proven difficult to produce an SIS mixer offering low-noise and wide-band characteristics[6].

We have developed an SIS mixer capable of tuning junction capacitance easily in the terahertz band, using the junction itself as a tuning circuit. This method makes use of a comparatively large SIS junction; this junction is treated as a distributed parameter line, while the resonator is fabricated with an elongated junction[7]. However, the operational bandwidth is limited by  $1/\omega C_j R_N$ , as in conventional SIS junctions, while wideband operation requires a junction featuring high critical current density. In this study, we focused on the distributed parameter tunnel junction, developing a tuning circuit offering a bandwidth ratio wider than  $1/\omega C_j R_N$  through the use of two or more resonant circuits.

### 3.1 Mixer design

As a mixer with a two distributed tunnel junction tuning circuit, we designed a quasi-optical mixer composed of a MgO hyper-hemispherical lens with a non-reflective layer (together forming the input optics) and a twin-slot antenna. Figure 9(a) shows a microphotograph of the mixer, and (b) shows an enlarged photograph of its tuning circuit component. The feed point of the twin-slot antenna was placed at the center of the tuning circuit part using a coplanar waveguide. The center frequency was designed to be 870 GHz, with antenna impedance of approximately  $65 \Omega$  in the vicinity of the center frequency[8][9]. The tuning circuit constituents were integrated to form a tuning circuit using a center conductor of one of the coplanar waveguides as a ground plane. The tuning circuit was equipped with a quarter-wave impedance transformer to match its impedance to that of the antenna. The mixer was produced by epitaxial NbN/MgO/NbN technology using a single crystal MgO substrate, and the tuning circuit was constructed with a NbN/MgO/NbN tunnel junction and a NbN/MgO/NbN microstrip line[10][11].

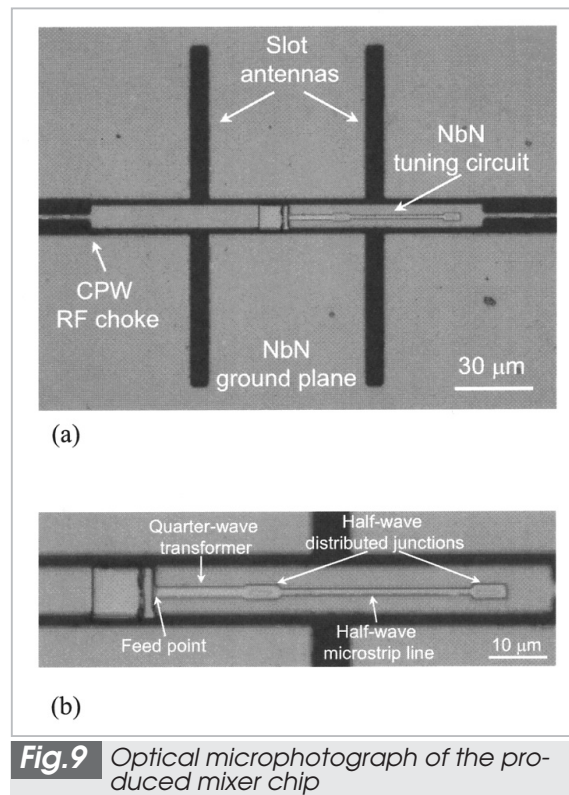


**Fig.9** Optical microphotograph of the produced mixer chip

The tuning circuit was designed such that the gain in the ratio of bandwidth to that of the center frequency would be 20% (174 GHz), with reflection loss of  $-10$  dB or less, based on analysis results using a simple circuit model. Table 1 shows the parameters used in the design. These values were mainly based on measured values, although the electrostatic capacitance of the epitaxial NbN/MgO/NbN junction per unit area was assumed to be equal to that of an epitaxially grown NbN/AlN/NbN junction[12]. Reference document[13] provides a detailed description of the method of calculating characteristic impedance and the propagation constants of the superconducting microstrip line and the SIS junction transmission line required in the design of the tuning circuit.

First, we attempted to determine the values for minimum critical current density required to satisfy the design requirements. Specifically,  $\alpha_j d_j$  values for a SIS transmission line  $1\text{-}\mu\text{m}$  wide at a center frequency of 870 GHz were plotted against critical current density, as shown in Fig.10. This figure shows that the critical current density satisfying  $\alpha_j d_j = 0.12$

**Table 1** Design parameters

NbN gap frequency	1.4 THz
normal state conductivity	$1.5 \times 10^6 \Omega^{-1}\text{m}^{-1}$
upper electrode thickness	400 nm
lower electrode thickness	200 nm
MgO insulator thickness	200 nm
dielectric constant	9.6
NbN/MgO/NbN $J_c R_N A$ product	3.5 mV
specific capacitance	$71 J_c^{0.16} \text{ fF}/\mu\text{m}^2$
MgO barrier thickness	1 nm

was found to be approximately  $16 \text{ kA}/\text{cm}^2$  ( $C_s = 110 \text{ fF}/\mu\text{m}^2$ ). Given that required critical current density is approximately  $40 \text{ kA}/\text{cm}^2$  in conventional designs, the obtained figure—less than half of this value—is likely to prove sufficient for the new tuning circuit.

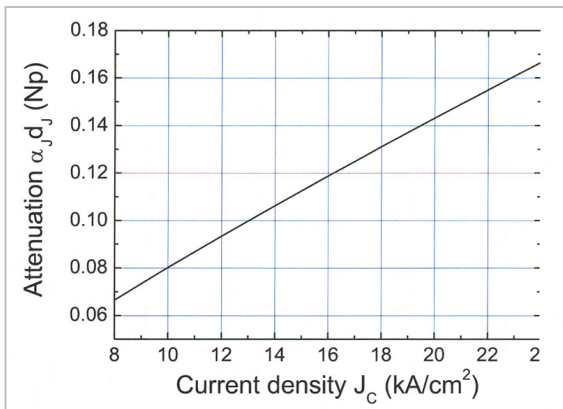
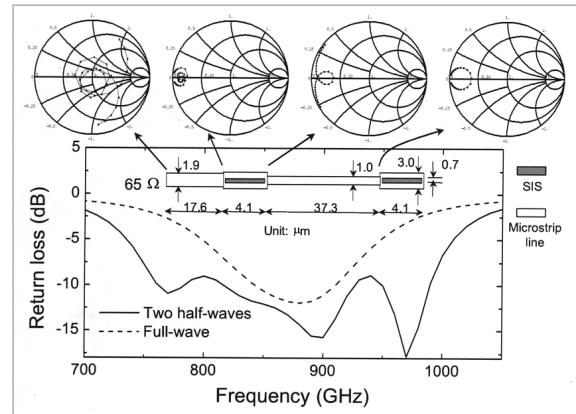
**Fig. 10** Dependence of propagation characteristics on critical current density in the SIS transmission line

Figure 11 shows a schematic diagram of the designed circuit and reflection loss with antenna impedance set to a constant value of  $65 \Omega$ . The figure also shows the impedance loci when viewing the load side from several points within the circuit. These are normalized with  $65 \Omega$ . The figure indicates that a reactance component having a frequency dependence of a half-wave junction (the junction is located at the termination) was well compensated for by the tuning circuit. Since the tuning circuit is equipped with a quarter-wave impedance transformer, the bandwidth ratio was wider than the design value, by more than 20%. In order to compare this circuit with a conventional tuning circuit, we calcu-

lated the reflection loss of a full-wave junction equipped with a quarter-wave impedance transformer featuring a total junction length equal to that of the two distributed tunnel junction tuning circuit at the same critical current density. As show by the dashed line in Fig.11, the bandwidth ratio is quite narrow, which indicates that the use of the two distributed tunnel junction tuning circuit is an effective means of lowering critical current density.

**Fig. 11** Schematic diagram of the tuning circuit and reflection loss

### 3.2 Evaluation of mixer performance

Performance of the fabricated mixer was evaluated using a quasioptical receiver system[14]. A mixer chip was attached to the back of the MgO hyper-hemispherical lens (radius of 3 mm) and was housed in a mixer block made of oxygen-free copper. In order to reduce surface reflection loss, the lens was coated with a non-reflective  $50\text{-}\mu\text{m}$ -thick layer of Kapton-JP polyimide film. A bandwidth ratio of approximately 75% at a center frequency of approximately 800 GHz was thus produced, with a reflection loss of  $-10 \text{ dB}$ . This band was significantly wider than that of the tuning circuit. The off-axis parabola mirror was arranged in a position to allow for the formation of a collimated beam, thus constituting the input optical system.

An intermediate frequency (IF) signal from the mixer was extracted by a balanced circuit and amplified with a 1.25- to 1.75-GHz cooled HEMT amplifier through a  $180^\circ$  hybrid

coupler. The IF signal was then amplified by a room temperature amplifier and detected through a bandpass filter of  $1.5 \text{ GHz} \pm 250 \text{ MHz}$ . The mixer block, the off-axis parabola mirror, a bias tee, the HEMT amplifier, and the hybrid coupler were attached to the cooling surface of a Dewar at 4.2 K. A backward oscillator (BWO) was used as a local oscillation wave (LO) source. The LO and RF signals were coupled by a Mylar film  $9\text{-}\mu\text{m}$  thick and made to enter the quasioptical mixer, after passing through a Teflon vacuum window  $0.5\text{-mm}$  thick and two thin Zitex sheets; these sheets were cooled to 77 K and 4.2 K, respectively. Noise temperature was evaluated by the standard Y-factor method. Specifically, black body radiation of two radio-wave absorber placed in room temperature (295 K) and one dipped in liquid nitrogen (77 K) are used as RF signal sources and these signals are input into the receiver. The ratio of IF output from the receiver to the value of these two inputs ( $P_{295}/P_{77}$ ) is deemed the Y-factor, which is then applied to determine the noise temperature of the receiver using the following formula.

$$R_{rx} = \frac{295 - Y \cdot 77}{Y - 1} \quad (2)$$

### 3.3 Mixer noise properties

Typical heterodyne responses of a receiver employing the two distributed tunnel junction tuning circuit are shown in Fig.12. The critical current density of the junction of a large area produced on the same substrate was found to be approximately  $6.7 \text{ kA/cm}^2$ . Since this junction has a low critical current density, the I - V characteristics with no LO input into the mixer are of high quality with a small sub-gap leak current, and the ratio between sub-gap resistance and normal resistance is large, at approximately 12. Because the superconductive material is NbN, the gap voltage is also large, at approximately 5.5 mV, equivalent to 1.34 THz—roughly twice the value seen with conventional Nb. At the gap voltage, the current shows an abrupt buildup of a quasiparticle current peculiar to the SIS junction,

and consequently it can be said that the junction features nearly ideal I - V characteristics. When an LO frequency of 690 GHz was input, a first-order photon-assisted tunneling step appeared among the I - V characteristics at approximately half of the gap voltage.

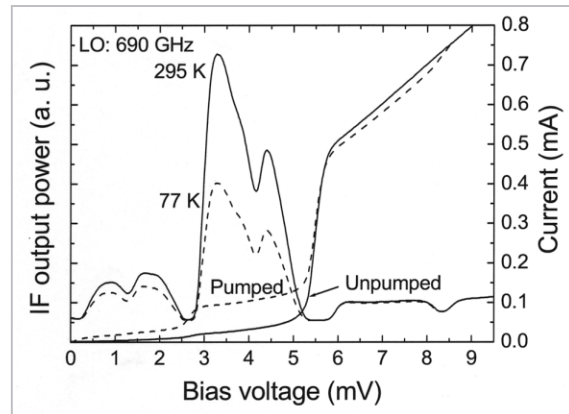
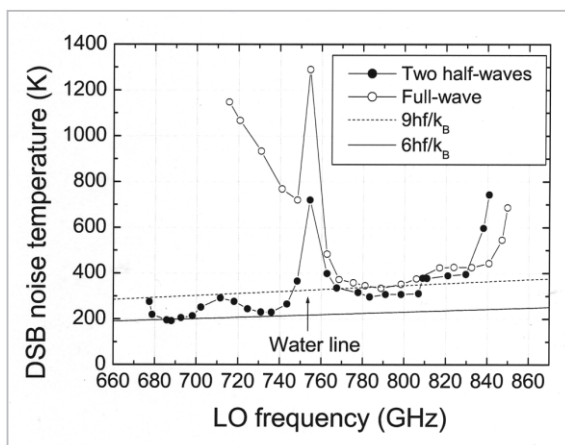


Fig. 12 Heterodyne response

Although the critical current density was lower than the design value, the receiver showed a large ratio of IF output to black body radiation input at 295 K and at 77 K, and a maximum Y-factor of 1.81 was obtained at a bias voltage of approximately 3.2 mV. Formula (2) shows this value to be equivalent to a double-sideband (DSB) receiver noise temperature of 192 K, corresponding to approximately 5.8 times quantum noise  $hf/k_B$ . It can be said that this value represents the best performance seen anywhere with the use of this frequency band, and is the result of the application of the high-quality I - V characteristics of a low critical current density junction.

Figure 13 shows the frequency dependence of receiver noise temperature measured by the same method. At frequencies from 675 GHz to 810 GHz, the receiver showed noise temperature nine times the quantum noise value (one and a half times the minimum noise temperature) or below. The bandwidth ratio was calculated at approximately 18%. Considering that the result of  $\omega C_J R_N$  using the parameters in Table 1 is approximately 23 at 750 GHz, the receiver clearly offers an extremely wide band. To facilitate comparison with a conventional tuning circuit, the

measurement results for receiver noise temperature of a full-wave junction produced on the same substrate is also shown in the figure. As predicted in design in the Section 3.2, the conventional tuning circuit has a narrow frequency band, whereas the proposed two distributed tunnel junction tuning circuit can operate in a wider frequency band with a junction of the same critical current density. Therefore, it can be said that this tuning method offers an effective means of lowering the critical current density of the junction.



**Fig. 13** Frequency dependence of receiver noise temperature

However, the actual operating center frequency was lower than the designed center frequencies—by approximately 14% in the two-junction tuning circuit and approximately 7% in the full-wave tuning circuit—and thus a problem was inferred in the setting of the design parameters. Because the center frequency of the full-wave tuning circuit is mainly governed by the resonance frequency of the distributed SIS tunnel junction transmission line, it is safe to conclude that the phase velocity of the junction transmission line itself was slower than the design value. Moreover, because the two-junction tuning circuit was slow in operating frequency, it was concluded that the phase velocity of the microstrip line was also slower than the design value. Another

possible cause lies in the magnetic penetration depth of NbN, which may be larger than the design value calculated by the Mattis-Bardeen theory. We are now proceeding to detailed evaluation of these factors, and will redesign the tuning circuit accordingly [15]-[17].

## 4 Conclusions

To improve the high-frequency properties of the thin-film-resistance-shunted Josephson junction to be used in the Josephson array oscillator, we devised a Josephson junction structure that minimizes parasitic inductance  $L_s$  in the process succeeding in reducing parasitic inductance  $L_s$  to approximately 100 fH through analysis based on computer simulation. This junction is used to produce 650-GHz and 1-THz Josephson array oscillators experimentally, and we detected values of approximately  $10 \mu\text{W}$  at 625 GHz and approximately  $50 \text{ nW}$  at 1 THz. These experiments have shown that by changing the thin film material to be used in the microstrip resonator to a material offering lower loss in the terahertz band, it will be possible to construct a THz Josephson oscillator delivering practical oscillation output.

In order to realize an SIS mixer with low-noise, wideband characteristics in the terahertz band, we proposed and developed the two distributed tunnel junction tuning circuit, which employs a junction with low critical current density and high-quality I - V characteristics. We then produced an all-NbN mixer using epitaxial NbN/MgO/NbN technology, evaluated its performance, and demonstrated its low-noise and wide band properties in the 800-GHz band. This tuning circuit is theoretically capable of low-noise and wide-band operation up to about 1.4 THz (the gap frequency of NbN), and is believe to hold a great deal of promise in applications involving high-performance mixers in the terahertz band.

---

## References

- 1 K. Hara, "Superconductive electronics", Ohmsha, p. 128, 1985.
- 2 A. Kawakami and Z. Wang, "Josephson Array Oscillator Using Resonant Effects in Shunted tunnel Junctions", *IEICE Trans. Electron.*, Vol. E79-C, No. 9, pp. 1242-1246, Sep. 1996.
- 3 A. Kawakami, Y. Uzawa, and Z. Wang, "Josephson Array Oscillators with Microstrip Resonators," *IEEE Trans. Appl. Supercond.* Vol. 7, pp. 3126-3129, Jun. 1997.
- 4 J. Carlstrom and J. Zmuidzinis, "Millimeter and submillimeter techniques", in *Review of Radio Science 1993-1996*, W. Ross Stone, Ed. Oxford: The Oxford University Press, 1996.
- 5 S.-C. Shi and T. Noguchi, "Low-noise superconducting receivers for millimeter and submillimeter wavelengths", *IEICE Trans. Electron.*, Vol. E83-C, pp.1584-1594, 1998.
- 6 B. D. Jackson, G. de Lange, W. Laauwen, J. R. Gao, N. N. Josad, and T. M. Klapwijk, "NbTiN/SiO<sub>2</sub>/NbTiN and NbTiN/SiO<sub>2</sub>/Al tuning circuits for 1 THz waveguide SIS mixers", in *Proceeding of the 11th International Symposium on Space Terahertz Technology*, University of Michigan, Ann Arbor, MI, 1-3 May 2000 (unpublished).
- 7 Y. Uzawa, A. Kawakami, S. Miki, and Z. Wang, "Performance of all-NbN quasi-optical SIS mixers for the terahertz band", *IEEE Trans. Appl. Supercond.*, Vol. 11, pp. 183-186, 2001.
- 8 J. Zmuidzinis, N. G. Ugras, D. Miller, M. Gaidis, H. G. LeDuc, "Low-noise slot antenna SIS mixers", *IEEE Trans. Appl. Supercond.*, Vol. 5, pp. 3053-3056, 1995.
- 9 M. Gaidis, H. G. LeDuc, M. Bin, D. Miller, J. A. Stern and J. Zmuidzinis, "Characterization of low-noise quasi-optical SIS mixers for the submillimeter band", *IEEE Trans. Microwave Theory Tech.*, Vol. 44, pp.1130-1139, 1996.
- 10 A. Kawakami, Z. Wang, and S. Miki, "Low-loss epitaxial NbN/MgO/NbN trilayers for THz applications", *IEEE Trans. Appl. Supercond.*, Vol. 11, pp. 80-83, 2001.
- 11 A. Kawakami, Z. Wang, and S. Miki, "Fabrication and characterization of epitaxial NbN/MgO/NbN Josephson tunnel junctions", *J. Appl. Phys.*, Vol. 90, pp. 4796-4799, 2001.
- 12 Z. Wang, Y. Uzawa, and A. Kawakami, "High current density NbN/AlN/NbN tunnel junctions for submillimeter wave SIS mixers", *IEEE Trans. Appl. Supercond.*, Vol. 7, pp. 2797-2800, 1997.
- 13 Y. Uzawa and Z. Wang, "Studies of High Temperature Superconductor", ed. A. V. Narliker (Nova Science, Hauppauge, NY, 2002) Vol. 43, Chap. 9, p. 255.
- 14 Y. Uzawa, Z. Wang, and A. Kawakami, "Performance of quasi-optical SIS mixer with NbN/AlN/NbN tunnel junctions and NbN tuning circuit at 760 GHz", *Appl. Supercond.*, Vol. 6, pp. 456-470, 1998.
- 15 A. Kawakami, Y. Uzawa, and Z. Wang, "Specific capacitance of epitaxial NbN/MgO/NbN tunnel junctions for THz applications", to be published in *Appl. Phys. Lett.*
- 16 A. Kawakami, Y. Uzawa, and Z. Wang, "Measurement of capacitance and penetration depth in NbN/MgO/NbN junctions", *Proc. the 64th Japan Society of Applied Physics and Related Society*, 31a-A-5, p.213, 2003.
- 17 Y. Uzawa, M. Takeda, A. Kawakami, and Z. Wang, "A tuning circuit with two half wave-length junctions for SIS mixers", *Proc. the 64th, Japan Society of Applied Physics and Related Society*, 31a-A-7, p.214, 2003.



**WANG Zhen, Ph. D.**

*Leader, Superconductive Electronics Group, Basic and Advanced Research Department*

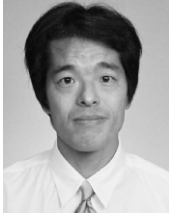
*Superconductive Electronics*



**KAWAKAMI Akira, Ph. D.**

*Senior Researcher, Superconductive Electronics Group, Basic and Advanced Research Department*

*Superconductive Electronics, Device Fabrication Process.*



**UZAWA Yoshinori, Ph. D.**

*Senior Researcher, Superconductive Electronics Group, Basic and Advanced Research Department*

*Development of Superconducting Receiver Technologies in the Submillimeter-wave band*

